A Numerical Solution for the Single-Screw Extrusion of a Polymer Melt

DAVID F. DYER

Auburn University, Auburn, Alabama

A general numerical-analysis procedure is presented for the screw extrusion of a non-Newtonian material. The full Navier-Stokes energy and continuity equations are used in the numerical procedure. The flow is taken as steady and incompressible, and the viscosity is written according to the Ostwald-de Waele model in which the viscosity is assumed to be inversely proportional to the square root of the second invariant of the rate of deformation tensor and exponentially dependent on the temperature.

The procedure allows the prediction of vorticity, stream-function, swirl velocity, internal energy, and viscosity over any cross section of a groove containing plastic. Calculations for the mass extrusion rate and power consumption (shear rate) for the screw extruder are also given. Typical cases are considered for which all the quantities listed above are determined. The results compare favorably with other theoretical work.

Past consideration of melt processing of thermoplastics is focused to a great extent on the prediction of the relationship between stress and rate of strain (equation of state) applying to a given material. Nontrivial solutions must be developed which utilize such equations of state to assess the merits of any proposed equation of state. The best representation for an equation of state can only be found by comparing the results of its use in a comprehensive solution with the experimental data. Obviously it is desirable to employ the most comprehensive solution possible consistent with an acceptable amount of computing expense. The comprehensive solution can also be used to check the accuracy of simpler solutions which can be effected with a minimum of computing time.

The present discussion is restricted to the most important example of melt processing, namely, the single-screw extruder which is diagramatically shown in Figure 1. The barrel is driven by a motor while the screw is held fixed. Generally, solid polymer is fed at a constant rate into the feed section from the hopper. The screw forces the material into the compression section where viscous shear causes the material to melt. The molten polymer is then pumped through the metering section and finally through a die or orifice to form the desired product shape. The usual screw extruder operates with a constant height of material in the hopper so that the extrusion rate is controlled chiefly by the pumping action of the metering section. Under these conditions, a steady, stable operation is achieved.

The objective of this paper is to obtain a comprehensive solution for the pumping phenomena in the metering zone of a single-screw extruder. The paper is not concerned with the design of extrusion apparati or with determining equations of state for polymers; rather it is desired to develop a solution scheme which is capable of accounting for all the phenomena occurring in the metering zone. A comprehensive solution of this type has not been reported in previous literature. As indicated earlier, this solution can be used to check the validity of equations of state and simpler solutions.

Pearson (*1*) presents a monograph concerned with many polymer melt processing systems (including the single-screw extruder) in which he considers two fundamental aspects: representations of the equation of state for polymers, and description of the fluid mechanics of melt processing. He cites the significant contributions in these areas up to 1966; consequently, a detailed review of this work would be superfluous. Pearson presents a calculation procedure which is typical of those previously reported in the literature for the metering section in a single-screw extruder. The chief assumptions are: (a) convection contributions are negligible (that is, the lubrication approximation is made); (b) side wall effects are absent; (c) the channel around the screw is unrolled (that is, the channel is assumed straight so that curvature effects are neglected); and (d) the effect of flow (and shear) between the flight tips and barrel is neglected. Under certain conditions, any (or all) of these assumptions may be invalid. Typical results of this procedure are also given elsewhere (*1*).

MATHEMATICAL MODEL

Figure 2 shows a cross section through a groove in the screw and defines the coordinates, dimensions, and velocities which are to be used in the following analysis. Cylindrical coordinates are used. The effect of the helical grooves is to produce a velocity at the barrel surface in both the θ and z directions. Since the velocities at the screw surfaces are zero, it is not necessary to consider the effect of the helix angle on these boundary conditions. Coordinates are taken with reference to the screw.

The density of the polymer is assumed constant in accordance with experimental evidence. As a result of the relatively small variations in temperature, the specific heat of the polymer is also taken as a constant. The viscosity is assumed to be functionally dependent on temperature. The analysis will be made for the continuous operation period so that the flow will be essentially steady.

Thus, in the present solution, three of the four major assumptions of most previous solutions are eliminated; namely, convection, side wall, and curvature effects are included. The fourth effect (flow between the flight tips and barrel) is not included, but the solution scheme employed in this paper could be easily extended to include this effect by taking the grid used for numerical calculation

to include the area between the flight tips and barrel.

GOVERNING EQUATIONS

The equations governing the extrusion process (conservation of mass, momentum, and energy) can all be written in analogous form (2, 3)

$$\vec{G} \cdot \text{grad. } \phi = \text{div. } [\Gamma_\phi \text{ grad. } \phi] + S_\phi \qquad (1)$$

where ϕ is the conserved property, that is the dependent variable in the respective equations. For example, in the energy equation the internal energy is the conserved property. Spalding (3) derives the required conservation equations and shows how they can be made to fit the form of Equation (1).

Note that in the stream-function equation the left-hand side of Equation (1) is zero. Also, the first term on the right-hand side of Equation (1) for the case $\phi = \omega$ produces a simpler equation when it is written div.(Γ_ω grad. $\mu\omega$). These exceptions can easily be programmed in the numerical procedure discussed below.

For the present work, the following definitions for the conserved properties, ϕ, will be taken:

$$\omega = \frac{1}{r}\left(\frac{\partial v_r}{\partial z} - \frac{\partial v_z}{\partial r}\right) \qquad (2)$$

$$r\rho v_z = \frac{\partial \psi}{\partial r}; \quad r\rho v_r = -\frac{\partial \psi}{\partial z} \qquad (3)$$

$$v_\theta = v_\theta \qquad (4)$$

$$u = CT \qquad (5)$$

Vorticity is usually considered to be a vector quantity. The definition given above is the θ component of the vorticity vector. Subsequently, this component will be called the *vorticity*. Equation (1) for each of the conserved properties can be derived from the conservation laws of physics. For these definitions of the conserved properties, the exchange coefficients, Γ_ϕ, can be written as follows (where the exceptions noted above are considered):

$$\Gamma_\omega = 1 \qquad (6)$$

$$\Gamma_\psi = \frac{1}{r^2} \qquad (7)$$

$$\Gamma_{v_\theta} = \mu \qquad (8)$$

$$\Gamma_u = \frac{K}{C} \qquad (9)$$

and the source terms, S_ϕ, are as follows:

$$S_\omega = \left(\frac{\rho}{r^2}\right)\frac{\partial v_\theta^2}{\partial z} - \frac{2}{r}\left[\frac{\partial^2}{\partial r^2}\left(\mu\frac{\partial v_r}{\partial r}\right) - \frac{\partial^2}{\partial z^2}\left(\mu\frac{\partial v_z}{\partial z}\right) + \frac{1}{r}\frac{\partial}{\partial r}\left(\mu\frac{\partial v_z}{\partial r}\right) - \frac{\mu}{r^2}\frac{\partial v_z}{dr} + 2\frac{\partial^2}{\partial r \partial z}\left(\mu\frac{\partial v_z}{\partial z}\right) + \frac{1}{r}\frac{\partial}{\partial z}\left(v_r\frac{\partial \mu}{\partial r}\right)\right] \qquad (10)$$

$$S_\psi = \rho\omega \qquad (11)$$

$$S_{v_\theta} = -\frac{\rho v_r v_\theta}{r} - \frac{1}{r}\frac{dp}{d\theta} - \frac{v_\theta}{r}\frac{\partial \mu}{\partial r} - \frac{\mu}{r^2}v_\theta \qquad (12)$$

$$S_u = \mu\left[2\left(\frac{\partial v_r}{\partial r}\right)^2 + 2\left(\frac{v_r}{r}\right)^2 + 2\left(\frac{\partial v_z}{\partial z}\right)^2 + \left(r\frac{\partial}{\partial r}\left(\frac{v_\theta}{r}\right)\right)^2 + \left(\frac{\partial v_\theta}{\partial z}\right)^2 + \left(\frac{\partial v_z}{\partial r} + \frac{\partial v_r}{\partial z}\right)^2\right] \qquad (13)$$

BOUNDARY CONDITIONS

Boundary conditions for each of the four conserved properties must be specified on all four of the walls bounding the polymer flow. The boundary conditions employed, along with a discussion of their derivation, is presented below.

Vorticity

To obtain the general equation for the boundary condition on the horizontal walls, consider a horizontal wall moving at a velocity U. Along this wall, $v_r = 0$ so that $\partial v_r/\partial z = 0$. Then, from its definition, the vorticity at the wall (point B) is

$$\omega_B = -\frac{1}{r}\frac{\partial v_z}{\partial r}\Big]_B \qquad (14)$$

A one-dimensional analysis near the wall provides the appropriate approximate expression for the velocity profile, namely

$$v_z = A[r - r_B] + \frac{1}{2}B\,[r^2 - r_B^2] + U \qquad (15)$$

By definition,

$$\frac{\partial \psi}{\partial r} = r\rho v_z \qquad (16)$$

Substitution of Equation (15) into Equation (16) with an integration from point B to n (where n is a neighboring point) gives

$$\psi_n = AC_1 + BC_2 + UC_3 \qquad (17)$$

where

$$C_1 \equiv \left[\frac{r_n^3 - r_B^3}{3} - \frac{r_B(r_n^2 - r_B^2)}{2}\right]\rho \qquad (18)$$

$$C_2 \equiv \left[\frac{r_n^4 - r_B^4}{8} - \frac{r_B^2(r_n^2 - r_B^2)}{4}\right]\rho \qquad (19)$$

$$C_3 \equiv \left[\frac{r_n^2 - r_B^2}{2}\right]\rho \qquad (20)$$

and ψ_B is set equal to zero. The vorticity at points B and n can be written:

$$-\omega_B = \frac{A}{r_B} + B \qquad (21)$$

$$-\omega_n = \frac{A}{r_n} + B \qquad (22)$$

Elimination of A and B by solving Equations (17) and (22) simultaneously, upon substitution into Equation (21), yields

$$\omega_B = \omega_n - \frac{(r_B - r_n)}{r_B}\,\frac{\psi_n + r_N\omega_n C_1 - UC_3}{C_2 - C_1 r_n} \qquad (23)$$

Equation (23) is the expression for the boundary condition along the horizontal wall of the screw and the barrel. Note that for the screw $U = 0$ while at the barrel $U = \Omega$. A similar analysis for a stationary vertical wall gives

$$\omega_B = \omega_n + \frac{(z_B - z_n)}{r_B}\,\frac{\psi_n - r_B^2 C_4\omega_n}{r_B C_5 - r_B C_4 z_n} \qquad (24)$$

where

$$C_4 = \left[\frac{z_B^2 - z_n^2}{2} - z_B(z_B - z_n)\right]\rho \qquad (25)$$

$$C_5 = \left[\frac{z_B^3 - z_n^2}{6} - z_B^2\,\frac{(z_B - z_n)}{2}\right]\rho \qquad (26)$$

Equation (24) can be used for either side wall of the screw.

Stream Function

Since there is no net flow between any of the solid boundaries, the stream function must have the same value on all the walls. Notice that the stream function does not represent the net amount of flow but is proportional to the net flow. For convenience, the boundary values are taken as zero. Hence, on all boundary walls to the flow,

$$\psi = 0 \tag{27}$$

Angular Velocity

The no-slip condition requires the angular velocity to be zero at the three screw walls and equal to the angular velocity of the barrel at the top wall; that is,

$$\begin{aligned} v_\theta &= 0 \quad \text{at screw surfaces} \\ v_\theta &= \Omega \quad \text{at top wall (barrel)} \end{aligned} \tag{28}$$

Internal Energy

Various boundary conditions can be used depending upon the problem to be considered. A practical case is considered in this paper in which the barrel temperature is taken as isothermal and the three screw walls are taken as adiabatic. Thus,

$$\begin{aligned} u &= CT_0 \quad \text{on barrel surface} \\ \frac{\partial u}{\partial \bar{n}} &= 0 \quad \text{at screw surface where } \bar{n} \text{ is the normal direction with respect to these surfaces.} \end{aligned} \tag{29}$$

where the reference temperature, T_0, is taken as the barrel temperature.

PROPERTY VALUES

Viscosity

Many polymers obey the Ostwald-de Waele viscosity model which can be written

$$\mu = 2\mu_0[I_2]^n \{\exp[b_0(T - T_0)]\} \tag{30}$$

where n is a constant and I_2 is the second invariant of the rate of deformation tensor which for the coordinate system used in this paper is

$$I_2 = \frac{1}{2}\left[\left(\frac{\partial v_r}{\partial r}\right)^2 + \left(\frac{v_r}{r}\right)^2 + \left(\frac{\partial v_z}{\partial z}\right)^2\right] + \frac{1}{4}\left[\left(r\frac{\partial}{\partial r}\left(\frac{v_\theta}{r}\right)\right)^2 + \left(\frac{\partial v_z}{\partial r} + \frac{\partial v_r}{\partial z}\right)^2 + \left(\frac{\partial v_\theta}{\partial z}\right)^2\right] \tag{31}$$

Other Properties

The values for the various required properties used in this paper are listed in Table 1.

NUMERICAL SOLUTION

The development of the desired solution involves solving Equation (1) subject to the boundary conditions given by Equations (23), (24), (27), (28), and (29). Spalding (3) proposes a scheme for solving a differential set of this type by a finite difference method. His method allows the simultaneous solution of an unlimited number of equations of the form of Equation (1) for an axially symmetric geometry. Spalding, et al. (4) develop Spalding's general formulation for three conserved properties, vorticity, temperature, and stream function, for an impinging jet and for the sudden enlargement of a stream in a pipe. They derive in detail the numerical formulation utilized and discuss the underlying reasons for the choice. Runchal, et al. (5) also discuss Spalding's formulation.

This paper is also a development of Spalding's proposal; however, it encompasses several features which are not discussed in (4). Chiefly, the new features of this paper lie in the fact that there are four conserved property equations, each interlinked quite strongly as a result of the dependence of viscosity on both temperature and rate of strain; perfect axial symmetry does not exist since there is a constant angular change in pressure. As a result of the discussion in (4), it will not be necessary to derive or discuss in detail the numerical formulation. However, for completeness, a summary of the method is given below.

The flow area is covered by a grid as shown in Figure 3. Conduction is assumed to pass through the sides of the tank surrounding P while convection takes place through the four tubes connecting point E, N, W, S with P. The formulation of the finite-difference expressions for Equation (1) is made with reference to this model. The conduction term is written in the usual manner for variable property heat conduction problems. The form suggested by Spalding (3) is

$$\text{div.}\,(\Gamma_\phi\ \text{grad.}\,\phi) = c_E\phi_E + c_N\phi_N + c_W\phi_W + c_S\phi_S - \phi_P\,(c_E + c_N + c_W + c_S) \tag{32}$$

where

$$c_E \equiv \frac{2b_{PE}/(z_E - z_P)}{(z_E - z_W)\,r_P} \tag{33}$$

$$c_W \equiv \frac{2b_{PW}/(z_P - z_W)}{(z_E - z_W)\,r_P} \tag{34}$$

$$c_N \equiv \frac{2b_{PN}/(r_N - r_P)}{(r_N - r_S)\,r_P} \tag{35}$$

$$c_S \equiv \frac{2b_{PS}/(r_P - r_S)}{(r_N - r_S)\,r_P} \tag{36}$$

where, $b \equiv r\Gamma_\phi$ and, for example, b_{PE} means the average value between points P and E.

The convection term of Equation (1) can be expanded in terms of the stream function. When the resulting expression is replaced in the finite-difference form suggested by Spalding (3) the following results

$$LHS = \frac{\dfrac{\frac{\psi_N + \psi_{NE}}{2} - \frac{\psi_S + \psi_{SE}}{2}}{r_N - r_S}\phi_{+P-E} - \dfrac{\frac{\psi_N + \psi_{NW}}{2} - \frac{\psi_S + \psi_{SW}}{2}}{r_N - r_S}\phi_{+S-P}}{(z_{PE} - z_{PW})rp} + \frac{\dfrac{\frac{\psi_E + \psi_{NE}}{2} - \frac{\psi_W + \psi_{NW}}{2}}{z_E - z_W}\phi_{+P-N} - \dfrac{\frac{\psi_E + \psi_{SE}}{2} - \frac{\psi_W + \psi_{SW}}{2}}{z_E - z_W}\phi_{+S-P}}{(r_{PN} - r_{PS})rp} \tag{37}$$

where, for example, ϕ_{+P-E} means that ϕ is evaluated at point P if its coefficient is positive and at point E if its coefficient is negative. In schematic form this expression

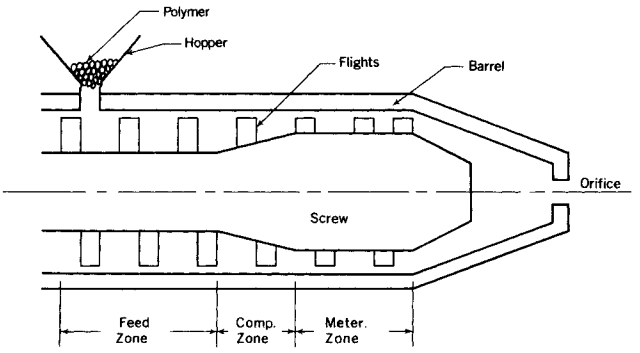

Fig. 1. Schematic diagram of single-screw extruder.

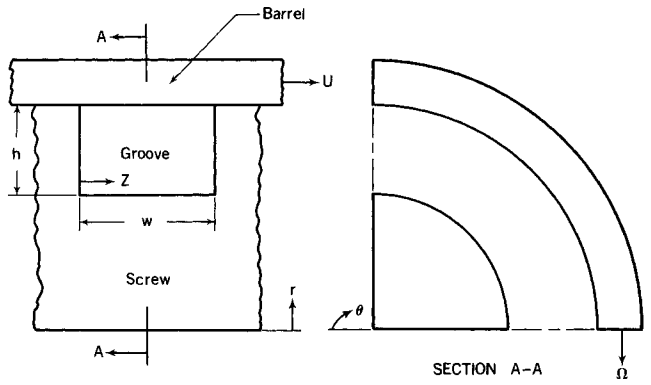

Fig. 2. Coordinate and Dimension diagram.

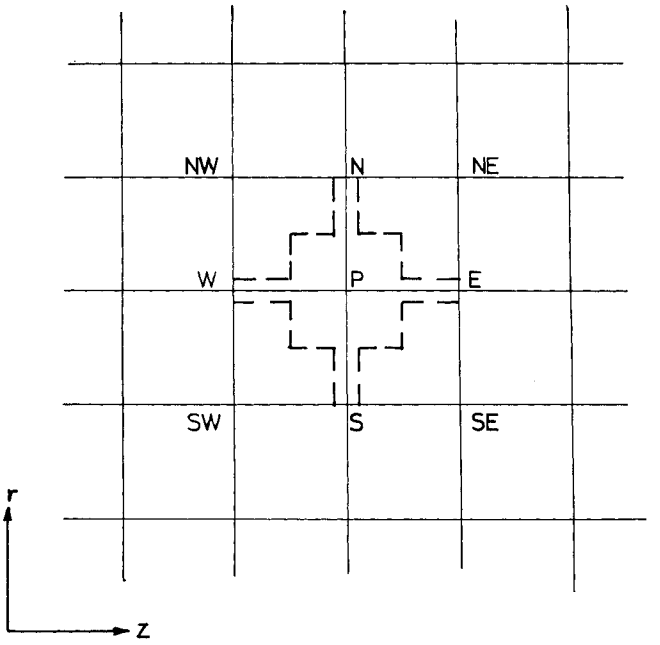

Fig. 3. Numerical grid network.

becomes

$$a_P\phi_P + a_E\phi_E + a_N\phi_N + a_W\phi_W + a_S\phi_S \qquad (38)$$

where the a's are defined by comparing the expressions given by Equations (37) and (38). Note that the particular definitions of the a's vary from point to point in the grid.

The source term, S_ϕ, can easily be expressed in a conventional center-difference formulation.

Thus, the complete expression for Equation (1) in finite-difference form is obtained by substituting the finite-difference formulations derived above for the respective terms in Equation (1). The result, expressed as a function of ϕ_P, is:

$$\phi_P = \frac{(c_E - a_E)\phi_E + (c_N - a_N)\phi_N + (c_W - a_W)\phi_W + (c_S - a_S)\phi_S + S_\phi}{a_P + c_E + c_N + c_W + c_S} \qquad (39)$$

One modification is made to Equation (39) for the case when $\phi = \omega$. Equations (23) and (24) show that for grid points next to a solid wall

$$\omega_B = D_1(\psi_n - UC_3) + D_2\omega_n \qquad (40)$$

where D_1 and D_2 are geometry functions. This dependence of ω at the boundary on internal values of stream function and vorticity can be incorporated directly into Equation (39) by defining two functions of position and conserved property, namely, $E(r, z, \phi)$ and $F(r, z, \phi)$. For $\phi = \omega$ and r, z lying on a solid boundary E and F are defined by

$$E_P = \frac{D_1(\psi_P - UC_3)}{\omega_B}$$

$$F_P = D_2$$

For all other cases $E = 1$, $F = 0$.

Equation (39) can be modified as follows to yield a general expression for ϕ_P

$$\phi_P = \frac{(c_E - a_E)\phi_E E_E + (c_N - a_N)\phi_N E_N + (c_W - a_W)\phi_W E_W + (c_S - a_S)\phi_S E_S + S_\phi}{c_E + c_W + c_N + c_S + (a_S - c_S)F_S + (a_E - c_E)F_E + (a_W - c_W)F_W + (a_N - c_N)F_N + a_P} \qquad (41)$$

Equation (41) is the algebraic substitution formula used in the integration technique. The main features of the computation procedure are as follows. Initial conditions are assumed and the boundary condition specified. The definition of stream function is used to calculate the velocity distribution and the viscosity is then calculated from the velocity gradients. Equation (41) is used to calculate new values of ϕ_P at each internal grid point. The maximum residual is calculated, and if the specified criterion for convergence is exceeded, iteration is performed as required.

DISCUSSION OF RESULTS

Computations were conducted for particular geometrical configurations using an IBM 7090 digital computer. The property values, screw dimensions, speed, and barrel temperature are given in the table. Results are obtained for the extrusion rate and torque for various pressure drops in the flow direction for two different cases as the table indicates. Representative values of Reynolds and Prandtl numbers for these cases based on the groove height, barrel tangential velocity and approximate value of viscosity in

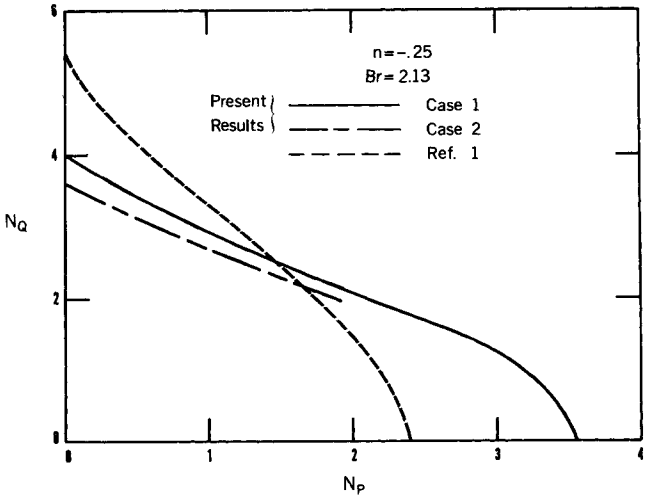

Fig. 4. Nondimensional flow rate vs. nondimensional pressure drop.

the center of the cross section are 3×10^{-4} and 8×10^{6} respectively. Case one was chosen to compare with the data given in (*1*) while case two was considered to show the effect of a different width-to-height ratio. In addition, the distribution of vorticity, stream function, swirl velocity, viscosity, and temperature over the groove section was obtained for all cases.

The convergence criterion, *CC*, was defined as follows:

$$CC = \frac{\phi_P{}^n - \phi_P{}^{n-1}}{\phi_P{}^n}$$

where the superscript n represents the number of the iteration. The maximum value of *CC* for each iteration and for each variable, ϕ, was calculated, and a sufficiently representative solution was assumed when this maximum value for all variables ϕ of a given iteration was less than 0.005.

The number of iterations required to achieve the desired accuracy increased from about 70 for $N_P = 0$ to 200 for $N_P = 3$. The computing time required on the IBM 7090 was of the order of 1.5 to 2.5 min.

It is impossible to nondimensionalize the governing equations in a manner which yields a single set of results for all situations. This is caused by the complexity of the equations considered. For the sake of comparison, the present results are nondimensionalized in terms of the parameters used in (*1*) which are a nondimensional pressure drop,

$$N_P = \frac{P_x(2h)^{2+2n}}{\mu_0\Omega^{1+2n}}$$

a nondimensional flow rate

$$N_Q = \frac{\dot{m}(\rho)}{\Omega h_w}$$

and a Brinkman number

$$N_{Br} = \frac{\mu_0(\Omega^{2n+2})h^{-2n}b_0}{(2^{1+2n})K}$$

Notice that the nondimensional flow rate is the ratio of the actual volume flow to that which would be achieved if all the flow moved at the barrel velocity, and the Brinkman number is a measure of the relative viscosity variation within the melt.

Table 1.

Properties	Case One	Case Two
pitch/diameter	1.0	1.0
b_o(1/°R.)	0.0068	0.0068
c (B/lb.$_m$°R.)	0.76	0.76
h (ft.)	0.00833	0.00833
K (B/hr.ft.°R.)	0.086	0.086
n	—0.25	—0.25
r (in.)	1.0	1.0
T_o (°R.)	760.0	760.0
U (ft./sec.)	0.737	0.737
W (ft.)	0.0698	0.0349
μ_o (lb.$_m$/ft. sec.$^{3/2}$)	4600.0	4600.0
ρ (lb.$_m$/cu.ft.)	47.0	47.0
Ω (ft./sec.)	0.21	0.21

In using these parameters to represent the results of this paper, it must be remembered that these results include at least three more effects than (*1*), namely, convection, curvature, and side wall effects. For example, the pressure drop is nondimensionalized in terms of the groove height. Certainly the groove width as well as the screw radius should be included for the more complex case. The main point is that it is impossible to represent the more comprehensive results in terms of a single set of dimensionless parameters; as a result, there is no known method of introducing additional parameters for this case into the existing nondimensionalizing quantities.

Figure 4 is a comparative plot of Q vs. N_P for cases one and two and (*5*). The deviation of the curves represents the refinement introduced by the more comprehensive solution since the variables Q and N_P are not altered for this solution in an attempt to account for the presence of additional effects. Case two which has the smaller width-to-height ratio shows a smaller Q for a given N_P than case one. This is the anticipated result since there is a greater relative side wall effect.

It is realized that the comparison shown in Figure 4 does not constitute a proof of the validity of the present method; however, the deviation is in line with what can be reasonably expected. Indeed, no absolute check of the validity of this method can be made analytically since this work is the most comprehensive analytical work currently available. The difficulty in using experimental data for a check lies in the fact that all substances would only approximately conform to the Ostwald-de Waele viscosity model. Indeed, this solution method can be used to check the applicability of various equations of state.

In addition to the data presented elsewhere (*1*), the dimensionless power consumption defined by

$$N_E = \frac{\text{Actual Power Consumed}}{\text{Power Consumed for a Linear Tangential Velocity Profile}}$$

was calculated for case one. The results are presented in Figure 5 and show the expected trend.

The distribution of conserved properties (ω, ψ, v_θ, U, μ) were calculated for both cases. The results show the expected trends. A short summary of the more important results is given below.

1. The stream function showed a recirculation pattern over the groove cross section which is induced by the axial movement of the barrel. The stream lines are shifted slightly towards the barrel for higher angular pressure gradients.

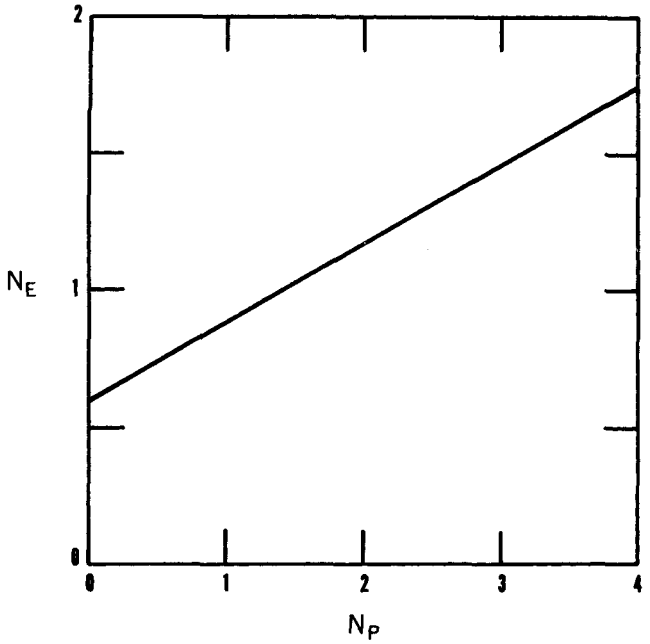

Fig. 5. Nondimensional shear rate vs. nondimensional pressure drop.

2. The angular velocity profile over the groove cross section shows that at a given height the angular velocity is constant over approximately the center 80% of the groove width. Each side wall exerts an influence in decaying the velocity over about 10% of the groove width. For $N_P = 1.83$ reverse flow in the θ-direction occurred near the surface opposite the barrel due to the retardation of the angular pressure gradient.

3. Due to the boundary conditions used for the energy equation (adiabatic screw walls and an isothermal barrel) the effect of viscous dissipation is easily seen from the temperature profiles. The maximum temperature in the polymer melt was about 3% higher than the wall temperature due to viscous dissipation.

4. The viscosity over most of the groove width increased exponentially from a value of about 150 $lb._m$/ft.-sec. at the barrel surface to a value at the screw surface of 250 $lb._m$/ft.-sec. for $N_P = 0$ and 450 $lb._m$/ft.-sec. for $N_P = 1.83$.

ACKNOWLEDGMENT

The author acknowledges with appreciation the aid of Professor D. B. Spalding, who suggested the problem and advised the author on the development of the method. Additionally, the work of A. K. Runchal and M. Wolfshtein toward development of the computer program is acknowledged. Dr. Williams and R. Fenner suggested appropriate fluid properties and typical geometry and operating conditions for the screw extruder.

This work is part of the author's postdoctoral study under a N.S.F. fellowship, directed by Professor D. B. Spalding at the Imperial College, London, England.

NOTATION

a_P, a_E, a_N, a_W, a_S = coefficients defined by comparing Equations (39) and (40), (lb./cu.ft.-sec.)ϕ*

A = constant in velocity profile Equation (15), (1/sec.)

b = product of exchange coefficient and radius, (ft.)Γ_ϕ

b_0 = viscosity temperature coefficient, (1/°R.)

B = constant in velocity profile Equation (15), (1/ft.-sec.)

C = specific heat, B.t.u./lb.°R.

c_E, c_N, c_W, c_S = coefficients defined by Equations (34), (35), (36), and (37), (1/sq.ft.)Γ_ϕ

C_1, C_2, C_3, C_4, C_5 = integration constants defined by Equations (18), (19), (20), (25), and (26)

CC = convergence criterion

$\vec{G}$ = mass flux vector, (lb./sq.ft.-sec.)

h = groove height, (ft.)

I_2 = second invariant of rate of deformation tensor, (1/sec.^{2})

K = thermal conductivity, (B.t.u./hr. ft. °R.)

$\dot{m}$ = mass flow rate extruded, (lb./sec.)

n = power dependence of viscosity on I_2

N_{Br} = Brinkman number

N_E = nondimensional power consumption

N_P = nondimensional pressure gradient

N_Q = nondimensional extrusion rate

r = radius, ft.

S = source term, Equations (10) through (13)

T = temperature, °R.

T_0 = reference temperature, °R.

u = internal energy, B.t.u./lb.

U = axial velocity of lid, ft./sec.

v = velocity, ft./sec.

W = groove width, ft.

z = axial coordinate, ft.

Greek Letters

Γ = exchange coefficient Equations (6), (7), (8), and (9), (1)Γ_ϕ

μ = viscosity, lb./ft.-sec.

μ_0 = strain coefficient of viscosity, lb./ft.-sec.$^{3/2}$

ρ = density, lb./cu.ft.

ϕ = conserved property, (1)ϕ

ψ = stream function, lb./sec.

ω = vorticity, 1/ft.-sec.

Ω = barrel tangential velocity, ft./sec.

Subscripts

B = at boundary wall

E = at nodal point east of considered point P

n = at neighboring point to wall

N = at nodal point north of considered point P

P = at considered nodal point

r = in radial direction

S = at nodal point south of considered point P

u = internal energy

v_θ = swirl velocity

W = at nodal point west of considered point P

z = in z direction

θ = in θ direction

ϕ = conserved property

ψ = stream function

ω = vorticity

* Where ϕ (or Γ_ϕ) is shown beside units in parentheses, the quantity when used in the equation for ϕ has the units of ϕ (or Γ_ϕ) times those shown inside the parentheses.

LITERATURE CITED

1. Pearson, J. R. A., "Mechanical Principles of Polymer Melt Processing," Pergamon Press, Oxford (1966).
2. Bird, R. B., W. E. Stewart, and E. N. Lightfoot, *Transport Phenomena*, pp. 101-105, John Wiley, New York (1962).
3. Spalding, D. B., "Notes on the Solution of the Navier-Stokes Equations for Steady Two-Dimensional Turbulent Flow by Numerical Techniques," Northern Research and Engineering Corporation, Cambridge, Mass. (Aug. 1966).
4. Spalding, D. B., A. K. Runchal, and M. Wolfshtein, *Rept SF/TN/2*, Imperial College, London (Aug. 1967).
5. Runchal, A. K., and M. Wolfshtein, *Rept. JF/TN/1*, Imperial College, London (July 1966).

Manuscript received March 22, 1968; revision received July 18, 1968; paper accepted July 26, 1968.